Journal of Thermal Analysis and Calorimetry, Vol. 97 (2009) 2, 403–407

EFFECT OF PRESSURE AND PARTICLE SIZE ON THE THERMAL CRACKING OF LIGHT CRUDE OILS IN SANDSTONE MATRIX

M. V. Kök[*]

Department of Petroleum and Natural Gas Engineering, Middle East Technical University, 06531, Ankara, Turkey

This research is focused on the effects of pressure (100-300 Pa) and matrix and on light crude oil combustion in sandstone matrix using pressurized differential scanning calorimetry (PDSC). Light crude oils and sandstone mixtures were prepared to give a composition of 15 mass% crude oil in sandstone matrix. A total of forty-eight PDSC experiments were performed. Roger and Morris kinetic model was used to analyse the data obtained from PDSC experiments and the results are discussed.

Keywords: *crude oil, DSC, kinetics, mesh size, pressure effect, thermal analysis*

Introduction

Thermal analysis is defined as including all techniques in which a physical property of a substance and/or its reaction products is measured as a function of temperature while the substance is subjected to a controlled temperature program. Analytical methods describing the thermal behavior of substances during programmed temperature changes, like thermogravimetry (TG/DTG), differential thermal analysis (DTA), or differential scanning calorimetry (DSC) are methods, which were applied at first to problems of inorganic chemistry, mainly to minerals. In recent years the application of thermal analysis techniques to study the combustion and pyrolysis behavior of fossil fuels has gained a wide acceptance among research workers, which is of exceptional significance for industry and for the economy.

Vossoughi [1] has used TG and DSC techniques to study the effect of clay and surface area on the combustion of selected oil samples. The results indicate that there was a significant reduction in the activation energy of the combustion reaction regardless of the chemical composition of additives. Moreover, the low-temperature oxidation of the oil and probably the coke deposition were strongly affected by the specific surface area of the solid matrix. From a series of isothermal TG mass-loss measurement on carefully selected combustion-tube samples, Wayland *et al.* [2] developed a set of curves that could identify the corresponding zones in the cores obtained from the field. Enthalpy measurements on the Athabasca oil sands and on the separated components in inert and in oxidizing atmospheres have been reported recently. Unfortunately there is a deficiency of similar data on crude oils in the literature. Thermal effects on the mineral and fluid content of an Athabasca oil sand sample were investigated by Bennion *et al.* [3]. The results showed that illite begins to degenerate at 475°C and kaolinite disappears at 625°C, while coke begins to form at 200°C. They claim that the changes observed in the oil and mineral composition could be used to monitor the thermal history of the reservoir and the path and location of an advancing fire front. Kamal and Verkocy [4] used TG and DSC on two Lloydminster region, heavy-oil cores, and extracted oils and mineral matter. TGA and DSC curves of two Lloydminster region cores and extracted oils obtained in helium and air atmospheres demonstrated at least three groups of chemical reactions occurring in three temperature regimes. Kök *et al.* [5–15] characterized the pyrolysis and combustion properties of crude oils. On combustion in air, three different reaction regions were identified, known as low-temperature oxidation, fuel deposition and high-temperature oxidation. DSC-TG/DTG curves have also been used to determine the heat values and reaction parameters of crude oil. Higher activation energy values were found as the API gravity of the crude oil decreased. Effect of clay and metallic additives are also studied. Lukyaa *et al.* [16] used pressurized differential scanning calorimetry to study the effects of sand particle size, pressure and oxygen partial pressure on the heat evolution during the combustion of North Sea crude-sand mixtures. They observed that decreasing particle size of the sand and increased pressure the extent of low-temperatures oxidation and thus favored fuel lay-down. Goncalves *et al.* [17] investigated the thermal behavior of asphaltenes from crude oil using thermal analysis techniques. The approach involves kinetic studies of the thermal

---

[*] kok@metu.edu.tr

1388–6150/$20.00

Akadémiai Kiadó, Budapest, Hungary
Springer, Dordrecht, The Netherlands

decomposition of asphaltenes under controlled conditions by thermogravimetry (TG/DTG). It was observed that the coke formed was also studied after being decomposed into smaller molecules using selective oxidation. Laux *et al*. [18] proposed that thermogravimetry proves to be an effective method for the determination of important parameters of processing of crude oil residues considering the influence of the colloidal character of these complex mixtures. Shiskin [19] used high-resolution differential scanning calorimetry to accurately establish the temperature intervals of oxidation/distillation of the major components of crude oils. The experimental TG-DSC curves show that the temperature scan of the run can be divided into six regions, of which the first belongs to simple distillation of the sample's liquid constituent (the distillate) and the others to oxidative cracking distillation of the solid (heavy) residue. The latter occur in the order paraffins+light oils, middle base oils, heavy base oils, condensed aromatics (resins) and asphaltenes. Li *et al*. [20] examined the oxidation, behavior of three crude oils (a light oil, a medium oil and an Athabasca bitumen) by using the pressurized differential scanning calorimeter (PDSC) at pressures from 110 to 6894 kPa. Pure hydrocarbon aromatics and paraffin samples were also selected for the current study. The study shows an increase of pressure results in an increase in the rate of oxidation reactions and heat released from the oxidation reactions. The PDSC heat flow curves also clearly demonstrate the effect of chemical structure of the samples on their oxidation behavior. The extent of oxidation of hydrocarbon samples is strongly dependent on the nature of the hydrocarbon.

Experimental

In this research, DuPont 2000 Thermal analysis system with PDSC modules was used. The PDSC system is a plug-in module which is capable of measuring temperature and heat flow associated with material transitions, providing quantitative and qualitative data on endothermic (heat absorption) and exothermic (heat evolution) processes.

Two light crude oils were mixed with two different sandstone samples at three different mesh size (40–50, 50–60 and 90–100). Using the PDSC, experiments were performed with a sample size of approximately 10 mg, at a heating rate of 10°C min^{-1} and at four different pressures (atmospheric, 100, 200 and 300 Pa) in the temperature range of 20–600°C. Prior to experiments, temperature calibration was performed. All the experiments were performed twice to see the reproducibility. Properties of crude oil and sandstone lithology are given in Table 1, respectively.

Results and discussion

Forty-eight PDSC experiments were performed in order to investigate the effect of pressure and mesh size on the oxidation behavior of crude oils in sandstone matrix. PDSC curves of for crude oil-1 in sandstone matrix at four different pressures (atmospheric, 100, 200 and 300 Pa) are given in Figs 1–4, respectively. In both

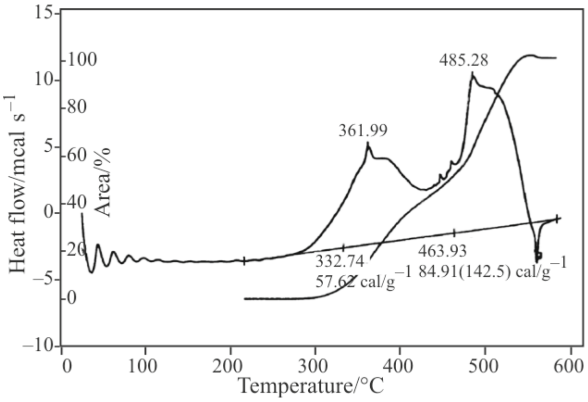

Fig. 1 PDSC curve of crude oil-1+(40–50) mesh sandstone-1 at atm. pressure

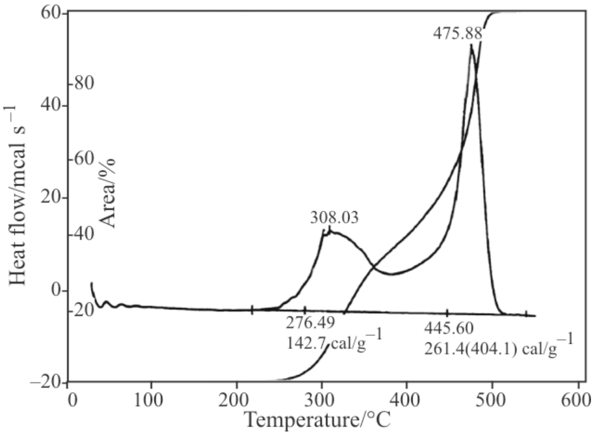

Fig. 2 PDSC curve of crude oil-1+(40–50) mesh sandstone-1 at 100 Pa

Table 1a Properties of crude oils

Crude oil	Viscosity (cp, at 20°C)	°API Gravity
Crude oil-1	3.6	30.1
Crude oil-2	11.7	31.5

Table 1b Properties of sandstone lithology

Properties	Sandstone-1	Sandstone-2
Silica/%	97	95.7
Iron-Alum/%	2.1	2.3
Calcium/%	0.7	1.2
Salts/%	0.01	–
Porosity/%	20	20

crude oil sanples in sandstone matrix, two distinct regions were identified known as low temperature oxidation (LTO) and high temperature oxidation (HTO). It was observed that as the pressure was increased, reaction temperatures are decreased whereas an increase was observed in the heating values of the samples. On the other hand heating values of the samples were increased as the mesh size increased. These trends can be explained by the fact that, increase in pressure will increase the amount of oxygen available for each reaction and hence the extent of reaction and heat evolved. Reduction in the size of sand particles will increase the packing within the sample, thus hindering diffusion of oxygen to the reaction site within the oil phase.

A kinetic method developed by Roger and Morris [21] gives a means of estimating activation energies from DSC curves. The recorded DSC data are in the form of distances between the curve and the baseline at the associated absolute temperature. This distance

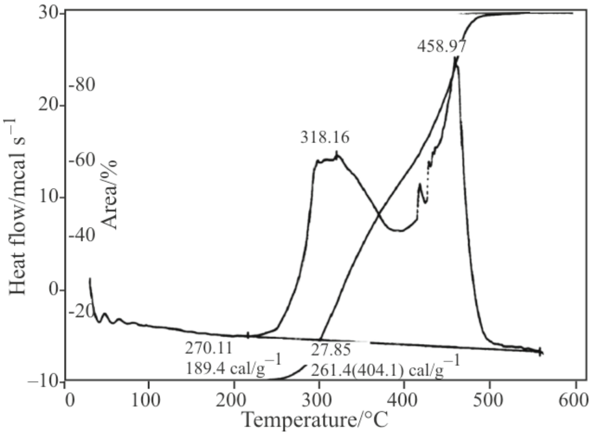

Fig. 3 PDSC curve of crude oil-1+(40–50) mesh sandstone-1 at 200 Pa

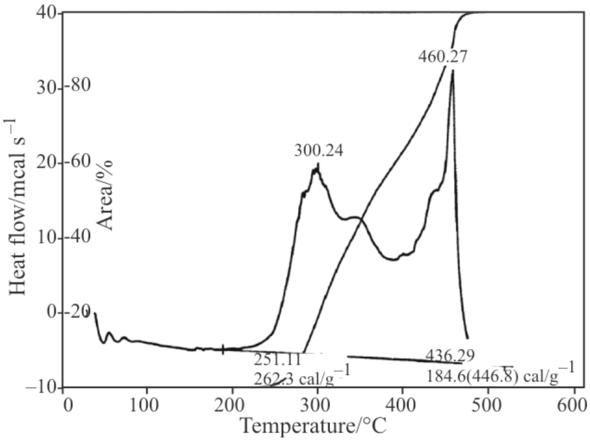

Fig. 4 PDSC curve of crude oil-1+(40–50) mesh sandstone-1 at 300 Pa

Table 2 Reaction parameters of the crude oil+sandstone samples

P/kPa	LTO Peak *T.*/°C	LTO *H.V.*/J g^{-1}	LTO *E*/kJ mol^{-1}	HTO Peak *T.*/°C	HTO *H.V.*/J g^{-1}	HTO *E*/kJ mol^{-1}	LTO+HTO Total *H.V.*/J g^{-1}
Crude oil-1+(40-50) mesh sandstone-1							
100	361.9	241.0	86.2	485.2	355.2	180.7	596.2
690	308.0	597.0	103.2	475.8	1093.7	170.7	1690.7
1380	318.2	884.0	63.9	458.9	792.4	110.5	1676.1
2070	300.2	1097.4	85.3	460.2	772.3	93.4	1869.4
Crude oil-1+(50-60) mesh sandstone-1							
100	364.1	394.1	78.6	480.4	450.6	85.6	844.7
690	348.3	1050.1	50.4	447.6	848.5	31.1	1899.1
1380	345.7	1215.0	46.6	456.8	882.8	24.7	2097.8
2070	306.5	1283.2	78.3	457.6	891.1	25.4	2174.4
Crude oil-1+(90-100) mesh sandstone-1							
100	393.3	487.0	25.7	506.3	441.8	30.2	928.4
690	360.9	1197.8	29.5	438.8	792.0	12.0	1989.9
1380	298.1	1228.8	105.6	446.1	830.9	30.3	2059.7
2070	300.5	1511.6	88.1	441.8	1053.9	20.5	2565.6
Crude oil-1+(40-50) mesh sandstone-2							
100	365.9	262.1	85.9	489.7	575.7	288.1	837.6
690	307.3	797.4	126.2	467.6	1135.1	107.8	1932.5
1380	311.7	905.4	76.2	469.6	1494.5	124.2	2399.9
2070	307.0	704.1	92.1	489.2	1325.0	178.8	2029.2

Table 2 contiuned

P/kPa	LTO Peak T./°C	LTO H.V./J g^{-1}	LTO E/kJ mol^{-1}	HTO Peak T./°C	HTO H.V./J g^{-1}	HTO E/kJ mol^{-1}	LTO+HTO Total H.V./J g^{-1}
Crude oil-1+(50-60) mesh sandstone-2							
100	368.2	295.6	72.5	490.4	483.6	217.9	779.4
690	359.3	870.6	41.9	461.0	1127.5	74.4	1998.2
1380	309.4	692.8	70.0	492.5	1500.8	234.2	2193.2
2070	314.9	707.5	62.6	492.9	1498.2	305.5	2205.8
Crude oil-1+(90-100) mesh sandstone-2							
100	392.8	425.0	51.6	487.0	492.8	63.4	917.9
690	306.2	1273.6	107.7	446.6	895.3	40.0	2169.4
1380	299.9	1451.0	103.1	442.0	1003.3	37.1	2454.3
2070	293.4	1526.3	111.7	437.3	1007.5	38.6	2533.4
Crude oil-2+(40-50) mesh sandstone-1							
100	358.6	147.7	69.2	499.1	410.0	136.4	557.7
690	315.6	569.4	87.6	482.1	1142.6	112.4	1712.0
1380	334.4	1028.4	63.7	448.9	661.4	48.1	1689.9
2070	340.0	1183.6	40.1	440.6	756.4	55.6	1940.1
Crude oil-2+(50-60) mesh sandstone-1							
		LTO			HTO		
100	366.1	254.6	60.7	486.0	619.2	202.1	873.6
690	340.7	1144.3	60.3	461.2	772.7	30.6	1916.6
1380	340.3	1004.1	46.0	457.9	705.0	35.3	1709.1
2070	324.1	1351.4	59.4	439.9	882.4	20.7	2233.8
Crude oil-2+(90-100) mesh sandstone-1							
100	366.3	378.3	57.2	483.3	638.9	68.0	1017.5
690	316.2	1244.7	80.2	456.4	756.0	18.1	2000.7
1380	315.5	1412.9	63.0	441.9	848.1	18.2	2261.0
2070	307.1	1567.7	75.2	437.2	941.4	14.6	2509.1
Crude oil-2+(40-50) mesh sandstone-2							
100	345.1	175.6	89.5	506.6	536.3	132.5	712.1
690	311.8	603.7	77.2	492.3	1376.9	119.2	1980.7
1380	327.8	1121.7	66.3	450.4	792.4	44.2	1913.7
2070	322.2	1163.1	74.0	447.7	782.8	36.9	1945.9
Crude oil-2+(50-60) mesh sandstone-2							
100	364.7	208.3	68.9	486.4	482.0	239.1	690.3
690	332.8	934.7	80.6	458.9	900.8	57.4	1835.5
1380	324.5	1159.8	67.8	448.0	802.4	40.7	1962.3
2070	310.2	1135.9	87.6	448.3	679.0	36.9	1815.0
Crude oil-2+(90-100) mesh sandstone-3							
100	368.3	364.0	62.1	486.0	623.4	98.3	987.4
690	317.5	1033.8	83.2	452.0	712.5	44.3	1746.8
1380	308.6	1316.7	77.7	445.2	848.9	40.0	2165.6
2070	300.6	1330.9	93.1	440.2	831.7	40.9	2162.7

P – pressure (kPa), *H.V.* – heating value (J g^{-1}), *E* – activation energy (kJ mol^{-1}), Peak *T* – peak temperature (°C) is proportional to the rate constant. The activation energy can be calculated from the following expression:

$$-E=R[(\ln D_1-\ln D_2)/(1/T_1-1/T_2)] \qquad (1)$$

where D_1 and D_2 are two distances from the baseline at the associated temperatures T_1 and T_2.

When the pressure was increased, it was observed that the activation energies and reaction temperatures generally decreased whereas, total heating values are increased. Another important point is observed in the change of mesh size. Decrease in sand particle size caused decrease in activation energies and increase in heating values (Table 2).

Acknowledgements

The authors would like to express their appreciation for the financial support of TUBITAK (The Scientific and Technological Research Council of Turkey) and OMFB (National Committee for Technological Development, Hungary).

References

1 S. Vossoughi, J. Thermal. Anal., 27 (1983) 17.
2 R. J. Wayland and D. O. Lee, Sandia National Lab. Report, Sand 83-0336, 1983.
3 D. W. Bennion and J. K. Donnely, Canada-Venezuela Oil sands Symposium, 1977, p. 139.
4 N. J. Kamal and J. Verkocy, J. SPE Reservoir Eng., (1986), 329.
5 M. V. Kök, Thermochim. Acta, 214 (1993) 315.
6 M. V. Kök, R. Hughes and D. Price, Thermochim. Acta, 214 (1996) 91.
7 M. V. Kök, R. Hughes and D. Price, J.Therm. Anal. Cal., 49 (1997) 609.
8 M. V. Kök and O. Karacan, J. Thermal. Anal., 52 (1998) 781.
9 M. V. Kök and G. Iscan, J. Therm. Anal. Cal., 64 (2001) 1311.
10 M. V. Kök, Energy Sources, 24 (2002) 1.
11 M. V. Kök, G. Pokol, C. Keskin, J. Madarasz and S. Bagci J. Therm. Anal. Cal., 75 (2004) 781.
12 M. V. Kök and C. Acar, J. Therm. Anal. Cal., 83 (2006) 445.
13 M. V. Kök, J. Therm. Anal. Cal., 84 (2006) 361.
14 M. V. Kök and G. Ýscan, J. Therm. Anal. Cal., 88 (2007) 657.
15 M. V. Kök, J. Therm. Anal. Cal., 90 (2007) 817.
16 A. B. A. Lukyaa, R. Hughes, A. Millington and D. Price, Trans. Inst. Chem. Eng., 72 (1994) 163.
17 M. L. A. Goncalves, M. A. G. Teixeira, R. C. L. Pereira, R. L. P. Mercury and J. R. Matos, J. Therm. Anal. Cal., 64 (2001) 697.
18 H. Laux, T. Butz and I. Rahimian, Oil and Gas Science and Tech., 55 (2000) 315.
19 Y. L. Shishkin, Thermochim. Acta, 440 (2006) 156.
20 J. Li, S. A. Mehta, R. G. Moore, E. Zalewski, M. G. Ursenbach and K. Van Fraasse, J. Canad. Petr. Tech., 45 (2006) 48.
21 N. Roger and E. D. Morris, Anal. Chem., 38 (1966) 412.

ICTAC 2008

DOI: 10.1007/s10973-008-9637-3